

where

$$\mathfrak{H}C_2' = \frac{1}{2}\hbar \sum_{\alpha \neq \beta} \mathfrak{F}_{\alpha\beta}(t) c_{\alpha}^* c_{\beta}, \quad (\text{A20})$$

and

$$\mathfrak{F}_{\alpha\beta}(t) = k_{\alpha\beta}'(P(t), Q(t)). \quad (\text{A21})$$

It follows from (A18) and (A21) that the statistical properties of  $\mathfrak{F}$  are determined by those of  $P$ ,  $Q$  that were discussed following Eq. (A18). One important quantity is  $\langle \mathfrak{F}_{\alpha\beta}(t) \rangle_{\text{ph}}$ . This is a constant, with respect to time, since we are considering only situations where the thermal conditions are steady. Therefore, by (A18) and (A21),

$$\langle \mathfrak{F}_{\alpha\beta}(t) \rangle_{\text{ph}} = \langle \mathfrak{F}_{\alpha\beta}(0) \rangle_{\text{ph}} = \langle k_{\alpha\beta}'(P, Q) \rangle_{\text{ph}}.$$

Consequently, by (A12) and (A15),

$$\langle \mathfrak{F}_{\alpha\beta}(t) \rangle_{\text{ph}} = 0. \quad (\text{A22})$$

It is convenient to re-express the formalism for  $\mathfrak{H}C'$  in terms of matrix elements between single-particle states

$$|\phi_{\alpha}\rangle = c_{\alpha}^* | \rangle,$$

where  $| \rangle$  is the vacuum state, i.e.,  $c_{\alpha} | \rangle = 0$  for all  $\alpha$ . It follows from (A9), (A13), (A19), and (A20) that

$$\mathfrak{H}C' = \mathfrak{H}C_0 + \mathfrak{H}C_1 + \mathfrak{H}C_2', \quad (\text{A23a})$$

where

$$\langle \phi_{\alpha}^* | \mathfrak{H}C_0 | \phi_{\beta} \rangle = \epsilon_{\alpha}' \delta_{\alpha\beta}, \quad (\text{A23b})$$

$$\langle \phi_{\alpha}^* | \mathfrak{H}C_1 | \phi_{\beta} \rangle = \frac{1}{2}\hbar \Omega_{\alpha\beta} (1 - \delta_{\alpha\beta}), \quad (\text{A23c})$$

and

$$\langle \phi_{\alpha}^* | \mathfrak{H}C_2' | \phi_{\beta} \rangle = \frac{1}{2}\hbar \mathfrak{F}_{\alpha\beta}(t) (1 - \delta_{\alpha\beta}). \quad (\text{A23d})$$

Also, by (A17), the dipole operator is given by

$$\langle \phi_{\alpha}^* | \mathbf{m} | \phi_{\beta} \rangle = -e_0 \mathbf{a}_{\alpha} \delta_{\alpha\beta}. \quad (\text{A24})$$

## Density and Energy of Surface States on Cleaved Surfaces of Germanium\*

D. R. PALMER, S. R. MORRISON, AND C. E. DAUENBAUGH

*Honeywell Research Center, Hopkins, Minnesota*

(Received 29 June 1962)

The channel technique has been successfully applied to measurement of the properties of cleaved germanium surfaces. A clean germanium surface is highly  $p$  type with the Fermi level near the valence band at the surface. This is brought about by acceptor-like surface states close to the edge of the valence band with a density of at least  $1.5 \times 10^{12}/\text{cm}^2$ . The density of these low-lying surface states decreases when the surface is exposed to oxygen. A comparison is made between results on cleaved surfaces and surfaces cleaned by ion bombardment.

IN recent years a number of attempts have been made to produce atomically clean surfaces on semiconductors. A clean semiconductor surface should lend itself to a much simpler and more fruitful investigation of basic surface properties.

A number of methods have been used to produce clean surfaces, namely, ion bombardment and annealing,<sup>1,2</sup> cleavage,<sup>3-10</sup> vacuum heat treatment,<sup>11-13</sup> and

hydrogen reduction.<sup>14</sup> Ion bombardment has been most widely used for studies<sup>15-20</sup> of the electrical properties of silicon and germanium surfaces because of the relative ease with which experiments can be done. How-

*tor Surface Physics*, edited by R. H. Kingston, (University of Pennsylvania Press, Philadelphia, 1957), p. 349.

<sup>9</sup> M. Green and K. H. Maxwell, *J. Phys. Chem. Solids* **13**, 145 (1960).

<sup>10</sup> D. R. Palmer, S. R. Morrison, and C. E. Dauenbaugh, *J. Phys. Chem. Solids* **14**, 27 (1960).

<sup>11</sup> J. T. Law and E. E. Francois, *J. Phys. Chem.* **60**, 353 (1956).

<sup>12</sup> F. G. Allen, J. Eisinger, H. D. Hagstrum, and J. T. Law, *J. Appl. Phys.* **30**, 1563 (1959).

<sup>13</sup> A. Kobayashi, Z. Oda, S. Kawaji, H. Arata, and K. Sugiyama, *J. Phys. Chem. Solids* **14**, 37 (1960).

<sup>14</sup> A. Kobayashi, and S. Kawaji, *J. Phys. Soc. Japan* **12**, 1054 (1957).

<sup>15</sup> P. Handler, in *Semiconductor Surface Physics*, edited by R. H. Kingston, (University of Pennsylvania Press, Philadelphia, 1957), p. 23.

<sup>16</sup> W. Portnoy, and P. Handler, Technical Note No. 2, University of Illinois, ASTIA Document No. AD-210-840, 1959 (unpublished).

<sup>17</sup> R. A. Missman and P. Handler, *J. Phys. Chem. Solids* **8**, 109 (1959).

<sup>18</sup> S. Wang and G. Wallis, *J. Appl. Phys.* **30**, 285 (1959).

<sup>19</sup> S. P. Wolsky and E. J. Zdanuk, *J. Phys. Chem. Solids* **14**, 124 (1960).

<sup>20</sup> R. Forman, *Phys. Rev.* **117**, 698 (1960).

\* This research was supported in part by the United States Air Force through the Air Force Office of Scientific Research (ARDC).

<sup>1</sup> H. E. Farnsworth, R. E. Schlier, T. H. George, and R. M. Burger, *J. Appl. Phys.* **26**, 252 (1955).

<sup>2</sup> R. E. Schlier and H. E. Farnsworth, in *Semiconductor Surface Physics*, edited by R. H. Kingston, (University of Pennsylvania Press, Philadelphia, 1957), p. 3.

<sup>3</sup> W. W. Scanlon, in *Semiconductor Surface Physics*, edited by R. H. Kingston (University of Pennsylvania Press, Philadelphia, 1957), p. 238.

<sup>4</sup> D. R. Palmer and C. E. Dauenbaugh, *Bull. Am. Phys. Soc.* **3**, 138 (1958).

<sup>5</sup> G. A. Barnes and P. C. Banbury, *Proc. Phys. Soc. (London)* **71**, 1020 (1958).

<sup>6</sup> G. W. Gobeli and F. G. Allen, *J. Phys. Chem. Solids* **14**, 23 (1960).

<sup>7</sup> D. R. Palmer, S. R. Morrison, and C. E. Dauenbaugh, *Phys. Rev. Letters* **6**, 170 (1961).

<sup>8</sup> M. Green, J. A. Kafalas, and P. H. Robinson, in *Semiconduc-*

ever, the cleavage technique can be used to produce an atomically clean surface which cannot be guaranteed by any other method.

It is possible to use a clean surface to investigate the effect of various gases on the properties of a surface in a controlled manner because the initial state of the surface should be reproducibly the same. We chose to use cleavage in ultra-high vacuum to achieve an atomically clean surface, at least temporarily. We have studied only the effect of adsorption and oxidation on the electrical properties of cleaved surfaces. Actual adsorption studies have been done separately by others<sup>8</sup> on germanium cleaved (crushed) surfaces.

From previous experiments<sup>10</sup> we found that a clean germanium surface produced by cleavage in high vacuum is highly *p* type with a field effect mobility of 100–300 cm<sup>2</sup>/V-sec. On exposure to oxygen,  $\sigma_s$ , the surface conductivity, initially increased by a small

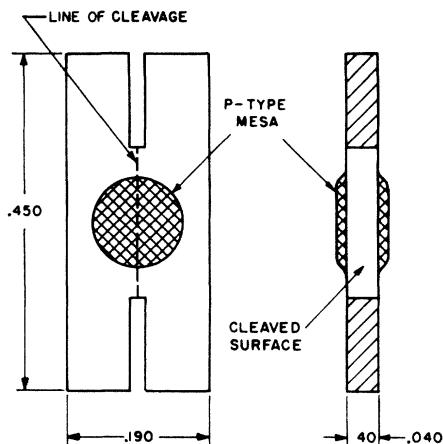


FIG. 1. Sample configuration

amount (more *p* type) and then decreased (more *n* type) until the surface eventually became *n* type. The field effect mobility increased to a maximum, then decreased, and eventually changed sign indicating an *n*-type surface. These experiments were performed on samples which were quite thick (1–2 mm) and had only one cleaved surface. The other surfaces were lapped or sandblasted. Although the results were qualitatively significant, we could not get good quantitative results because of poor sensitivity and because the surfaces, other than the cleaved surface, were not completely stable. These difficulties forced us to change our experimental approach.

If the surface is highly *n* or *p* type after cleavage, one can choose the bulk material so that an inversion layer is produced at the surface. It should then be possible to use the "channel" method of Statz and co-workers,<sup>21</sup> which effectively isolates the surface from the bulk,

<sup>21</sup> H. Statz, G. A. deMars, L. Davis, Jr., and A. Adams, Jr., Phys. Rev. **101**, 1272 (1956).

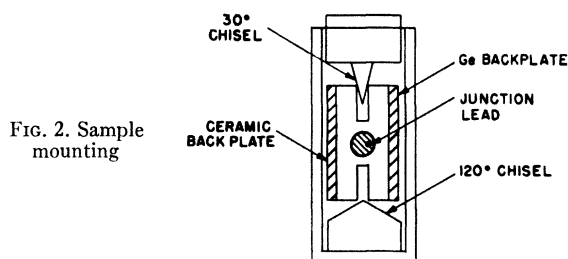


FIG. 2. Sample mounting

thus making it possible to measure surface conductivity directly. This method has already been used to study silicon cleaved surfaces.<sup>7</sup>

### EXPERIMENTAL TECHNIQUES

Since a cleaved germanium surface is initially highly *p* type, it is possible to produce an inversion layer on *n*-type germanium. Experiments were performed on a *pnp* transistor-like structure as shown in Fig. 1 with the specimen oriented for cleavage along a {111} plane. Junctions were formed by zinc diffusion and mesa etching. The surface concentration of the diffused layer was high enough to allow the use of a silver paste to make electrical contact to the junctions. The "base" was about 1 mm wide. Figure 2 shows the germanium sample, including back plates, as it was mounted in the sample holder. The backing plates were cemented to both sides of the sample to provide physical strength and proper orientation in the sample holder. Errors in sample dimensions are estimated at 5%. All measurements were room temperature.

The vacuum system was capable of reaching an ultimate vacuum of  $3 \times 10^{-9}$  mm Hg or less. Upon cleavage (by raising and dropping a magnetic hammer), an increase in pressure of about  $10^{-8}$  mm Hg was observed, although the pressure in the immediate vicinity of the cleaved surface was undoubtedly higher. The pressure dropped back to the initial pressure before cleavage in a matter of seconds. This burst in pressure had no apparent effect on our results.

A *p*-type inversion layer on *n*-type germanium is shown in Fig. 3 along with the measuring system. It is possible to isolate the surface from the bulk by application of reverse bias on the junctions so that channel resistance measurements can be made directly. However, if the ac impedance of the junctions is too small or the

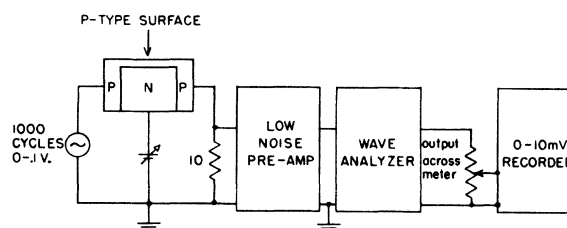


FIG. 3. Measuring system

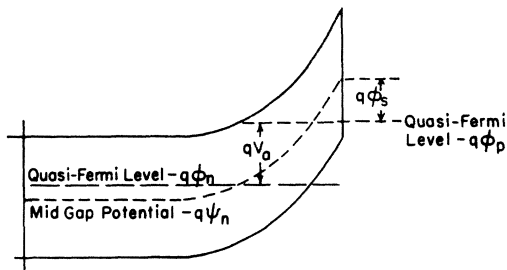


FIG. 4. Surface band structure showing inversion layer on *n*-germanium.

base resistance too large, an “unwanted” output is present. Since these conditions were not always met, we attempted to measure the base resistance and the ac impedance of the junctions to get an estimate of this “unwanted” output.

If a channel or inversion layer exists on the cleaved surface, one can determine the surface conductivity ( $\sigma_s$ ) as a function of reverse bias ( $V_a$ ) from measurement of the channel resistance. Figure 4 shows the position of the energy bands at the surface for a *p*-type inversion layer on *n*-type material.

Using the mathematical expressions of Statz and co-workers<sup>21</sup> and the surface mobility corrections as calculated by Schrieffer,<sup>22</sup> it is possible to determine  $\phi_s$  (the difference in energy between the center of the energy gap and the quasi-Fermi level for holes at the surface) and  $E_s$  (the electric field at the surface) as a function of  $V_a$ . The calculations are considered in more detail in the Appendix. From  $E_s$  the total charge in the space-charge region due to excess holes and ionized donors can be determined. This charge is equal in magnitude to the charge in the surface states but of opposite sign. This means we can determine the number of electrons in surface states. When a reverse bias is applied, some of the donors become ionized. These electrons are either taken up by surface states or re-

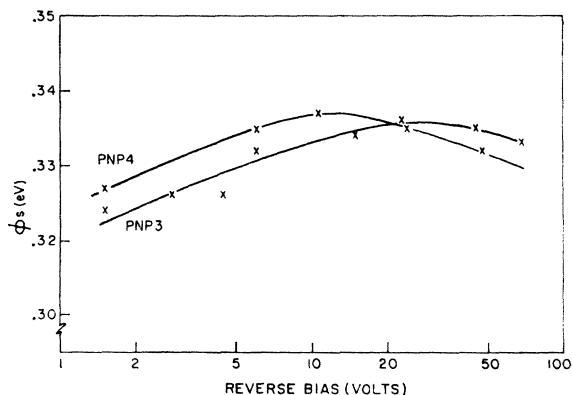


FIG. 5.  $\phi_s$  vs  $V_a$  immediately after cleavage, from samples *pnp3* and *pnp4*.

<sup>22</sup> J. R. Schrieffer, Phys. Rev. **97**, 641 (1955).

duce the excess hole density at the surface, thus lowering  $\phi_s$ .

From the measurements of  $\sigma_s$  vs  $V_a$ , the total charge in surface states can be determined as a function of  $\phi_s$ . In order to determine the charge in the “fast” states versus  $\phi_s$ , the charge in the “slow” states must be subtracted in a manner described by Statz *et al.*<sup>21</sup> However, we did not observe any slow-state effects in our experiments.

Through use of the usual Fermi distribution function to describe the occupancy of the surface states as a function of  $\phi_s$ , it is then possible to determine the energy and density of “fast” states.

## RESULTS

The first experiments were done using a “base” resistivity of  $7\Omega$  cm. After cleavage in ultra-high vacuum  $\sigma_s$  was about  $100 \mu\text{mhos/square}$  at 1.5 V reverse bias

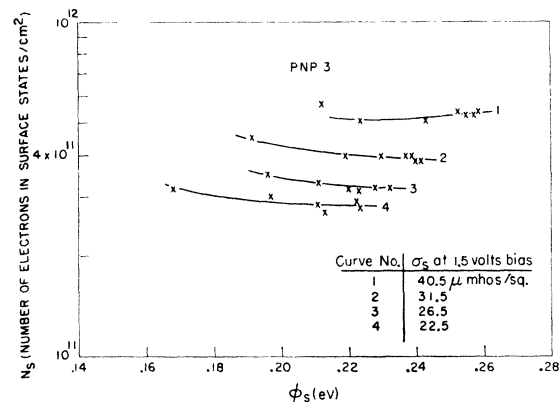


FIG. 6.  $N_s$  as function of  $\phi_s$ , sample *pnp3* (high  $\rho$ ). Curves 1-4 represent increasing oxygen exposure.

in three separate experiments. This meant that  $\phi_s$  was about 0.33 eV, or the Fermi level at the surface was near the edge of the valence band. The calculated values of  $\phi_s$  were obtained without taking into account the probable degeneracy of the surface.

It was not theoretically possible to change  $\phi_s$  or  $N_s$  (the number of electrons/cm<sup>2</sup> in surface states) by application of reverse bias immediately after cleavage, because the excess hole density was much larger than the change in density of ionized donors with applied field. For this reason it was not possible to determine explicitly the density and energy of surface states immediately after cleavage. However, the density of surface states must be at least  $1.5 \times 10^{12}/\text{cm}^2$ , the excess hole density at the surface. Figure 5 shows the calculated values of  $\phi_s$  as a function of  $V_a$  for two cleaved surfaces. The nonconstant value of  $\theta_s$  may indicate that the mobility corrections as a function of  $V_a$  are not quite correct. This also appears to be true at lower values of  $\phi_s$  where the surface is nondegenerate. An

increase in  $\phi_S$  at low-bias voltages was also observed by Statz *et al.*,<sup>21</sup> but was not interpreted in this manner.

After admission of oxygen to  $10^{-7}$  mm Hg,  $\sigma_S$  increased slightly (5–10  $\mu$ mhos/square) and then decreased, consistent with previous results<sup>10</sup> on conventional samples.

When  $\sigma_S$  had decreased from an initial value of about 100  $\mu$ mhos/square to about 40  $\mu$ mhos/square with oxygen exposure, it was possible to affect  $\phi_S$  by application of reverse bias. Figure 6 shows the calculated curves of the density of electrons in surface states,  $N_S$ , as a function of  $\phi_S$  on sample *pnp3*. These curves show essentially no change of  $N_S$  with  $\phi_S$ ; that is the density of charge in the states is independent of the Fermi level position over this variation of the Fermi level. Thus, there are few, if any, surface states over the range of  $\phi_S$  obtained, and the surface states under observation are filled. In this, and succeeding figures, the in-

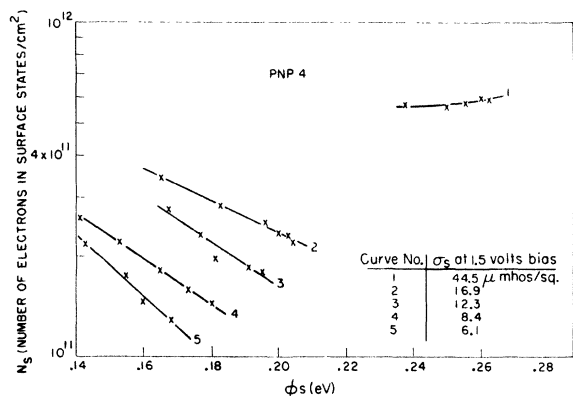


FIG. 7.  $N_S$  as function of  $\phi_S$ , sample *pnp4*, showing "annealing." Curve 1, a typical curve for before overnight evacuation. Curves 2–5, after overnight evacuation, with increasing oxygen exposure.

creasing numbers on the curves represent increasing oxygen exposure. Figure 7 shows the variation of  $N_S$  as a function of  $\phi_S$  on sample *pnp4*, with a history similar to *pnp3*. Here again, curve 1 is essentially flat, so  $N_S$  is constant. Curves 2–5 represent results obtained after an overnight evacuation of the system. These curves seem to indicate the presence of surface states somewhere near 0.16 eV. If these results are compared with those for *pnp3*, where we note no reasonable increase in charge on surface states as we approach  $\phi_S=0.16$ , it appears that surface states exist in this case of overnight "annealing" which were not present on sample *pnp3*. The possibility that surface states might have been generated by some slow reaction with oxygen exists but we were not able to substantiate this hypothesis.

Since it was not possible to change  $\phi_S$  by application of reverse bias immediately after cleavage using 7- $\Omega$ -cm germanium, it was necessary to use a lower "base" resistivity (0.14  $\Omega$ -cm). With the low-resistivity material

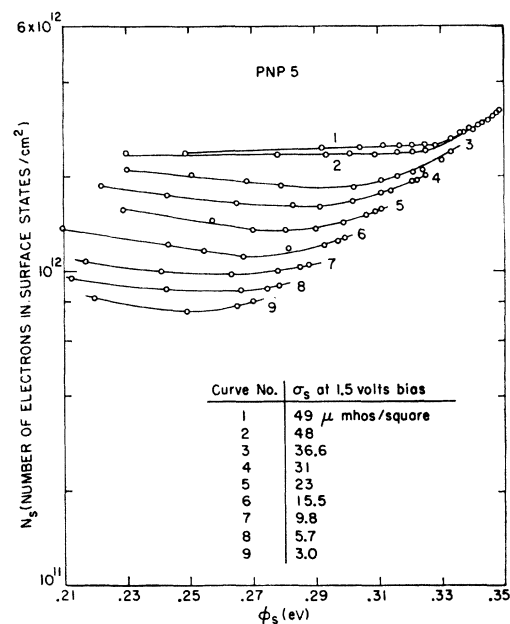


FIG. 8.  $N_S$  as function of  $\phi_S$ , sample *pnp5* (low  $\rho$ ).

it was possible to change  $\phi_S$  by application of reverse bias immediately after cleavage. Figure 8 shows curves of  $N_S$  vs  $\phi_S$  immediately after cleavage and after exposure to oxygen for sample *pnp5*. These results would indicate few, if any, surface states in the range from 0.2 to 0.34 eV below the center of the forbidden gap. Similar results are shown in Fig. 9 for sample *pnp6* (also 0.14  $\Omega$ -cm). These latter results are not in good agreement with those previously obtained, as these show an

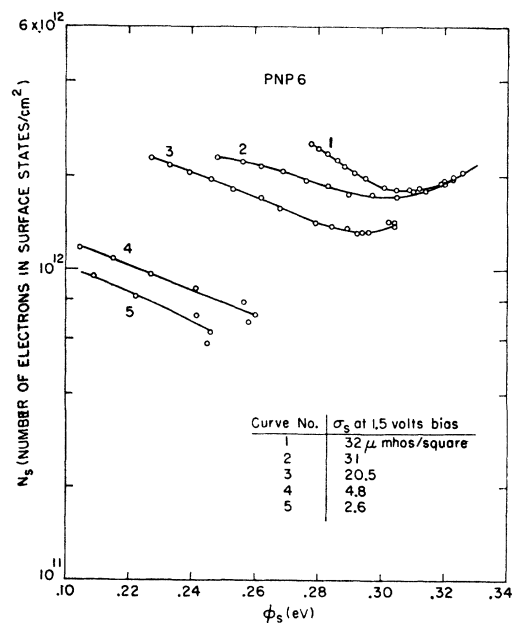


FIG. 9.  $N_S$  as function of  $\phi_S$ , sample *pnp6* (low  $\rho$ ).

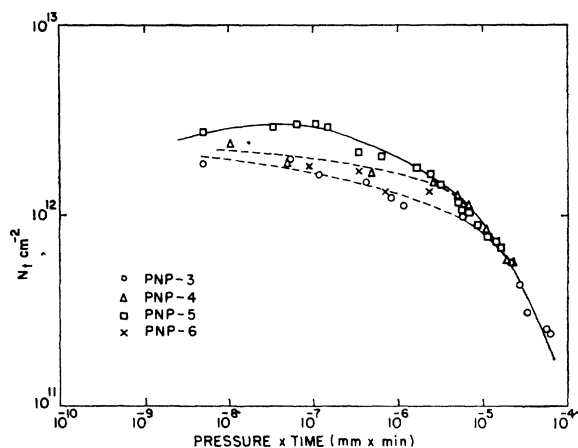


Fig. 10. Density of states on a germanium cleaved surface as function of oxygen history. Dashed lines indicate regions where insufficient data were available to calculate state density, and represent charge density on the surface,  $N_s$ . Squares correspond to sample *pnp5* (low  $\rho$ ), triangles and circles to *pnp4* and *pnp3*, respectively, (high  $\rho$ ), and  $\times$ 's to  $N_s$  on sample *pnp6* (low  $\rho$ ).

apparent variation in the charge with varying  $\phi_s$ . The manner of the change, with the charge density increasing with increasing  $\phi_s$ , over the high- $\phi_s$  region, does not appear to be physically interpretable, and it is possible that some experimental problem, such as a damaged surface, was involved. What we wish to emphasize with this plot is that the low-resistivity samples did not provide a uniformly reproducible result as did the high-resistivity samples. Obviously, of course, the results are qualitatively similar even in the questionable case.

Of additional interest is a logarithmic plot of  $N_t$  (the density of states) vs  $\phi_s$  for samples *pnp3*, *pnp4*, and *pnp5* as a function of pressure  $\times$  time shown in Fig. 10. In all cases the pressure was between  $10^{-9}$  mm Hg and  $10^{-5}$  mm Hg during oxygen exposure and were points taken within 6 h after cleavage. The data points from *pnp6* were included even though they did not indicate constant  $N_s$  with  $\phi_s$ . These data points represent the value of  $N_s$  as represented by the minimum of Fig. 10.

There is good agreement between the results of the different experiments. Also we note good agreement between values of  $N_s$ , the density of electrons, and  $N_t$ , the density of states. This apparent agreement is observed over several samples and over a wide range of oxygen pressure time. The consistency would tend to indicate that (a) the surface states are always filled in the conditions of this figure, (b) the value of  $N_t$  can be extrapolated to time zero, yielding a value for the density of states on a clean surface, and (c) the density is independent of the resistivity of the sample cleaved, with an energy near or below the edge of the valence band.

#### DISCUSSION OF RESULTS

Our results show that a cleaved germanium surface is initially *p* type with the Fermi level at the surface near

the edge of the valence band. This is brought about by acceptor-like surface states located near the edge of the valence band with a density of about  $2-3 \times 10^{12}/\text{cm}^2$ . The density of these states decreases in a reproducible manner upon exposure of the surface to oxygen.

$\Delta P$ , the excess hole density at the surface, as reported here, is in good agreement with results reported by Portnoy and Handler<sup>16</sup> and Forman<sup>20</sup> on clean surfaces produced by ion bombardment and annealing. On a cleaved surface  $\Delta P$  was  $2-3 \times 10^{12}/\text{cm}^2$ , with

$$\phi_s(v_{a=0}) = 0.33 \text{ eV},$$

as compared with the reported values of  $1.5 \times 10^{12}/\text{cm}^2$  and  $\phi_s = 0.31$  eV, by Portnoy and Handler, and  $10^{12}/\text{cm}^2$  by Forman. This agreement is surprisingly good considering the different methods used to obtain a clean surface. There is a greater difference, however, in the estimated density of surface states, which may be related<sup>20</sup> to the plane exposed.

The surface states responsible for the nearly degenerate surface produced by cleavage must be located near the edge of the valence band with a density of  $2-3 \times 10^{12}/\text{cm}^2$ , whereas Portnoy and Handler<sup>16</sup> determined from field effect and surface conductivity measurements that the density is at least  $8 \times 10^{12}/\text{cm}^2$  for a discrete trap at the Fermi level, and as large as  $8 \times 10^{13}/\text{cm}^2$  per eV for a uniform distribution in the forbidden gap. This would correspond to a factor of 2 discrepancy, allowing for the difference in surface state energy between his assumptions and our measurements. There is also qualitative agreement in the measured values of  $\sigma_s$  and  $\mu_{FE}$  for cleaved surfaces<sup>10</sup> and surfaces cleaned by ion bombardment and annealing.

The cleaved surfaces we obtained had steps and appeared somewhat curved so that our cleaved surfaces were far from atomically flat. Wolff and Broder<sup>23</sup> have shown that a fractured silicon surface is far from atomically flat even when it appears so on a macroscopic scale. Venables<sup>24</sup> has shown that cleavage splinters are formed at cleavage steps. Imperfect cleavage could certainly be expected to influence the reproducibility and validity of results obtained on cleaved surfaces. However, we have achieved good reproducibility using cleavage in conjunction with channel measurements initially after cleavage and after exposure to oxygen.

There can be little doubt that cleavage produces an atomically clean surface which cannot be guaranteed by any other method. Cleavage is very compatible with "channel" experiments whereas bombardment and annealing, or any other process involving heating, is not too feasible because the doping impurities used to form *p-n* junctions can be transferred to the surface being cleaned. Cleavage can be used on a wide variety of materials, limited only by the nature of cleavage.

<sup>23</sup> G. A. Wolff and J. D. Broder, *Acta. Cryst.* **12**, 313 (1959).

<sup>24</sup> J. D. Venables, *J. Appl. Phys.* **31**, 1503 (1960).

Although we chose to investigate the effect of oxygen on cleaved germanium surfaces, the effect of other gases could be studied equally as well. An area of interest, not cleared up in our experiments is the generation of surface states by oxygen at an energy closer to the center of the forbidden gap. It would be unreasonable to assume that new surface states are not generated by the adsorbed oxygen. Refinements in the cleavage technique, the ability to produce low leakage junctions, and an improved measuring system could allow more definitive information about germanium surfaces from "channel" experiments. It may also be possible, using the channel technique, to measure the effective mobility of holes at the surface by doing Hall-effect experiments.

#### APPENDIX

This section is included to show in more detail the method used to convert measurements of  $\sigma$  and  $V_a$  into  $\phi_s$  and  $N_s$ .

The starting point is the equations of Statz *et al.*<sup>21</sup>:

$$\left(\frac{\epsilon}{2\pi}\right)^{1/2} \frac{1}{q} \left[ \rho_d \left( |V_a| + |\psi_n| + |\phi_s| - \frac{kT}{q} \right) + \frac{kT}{q} q n_i \exp\left(\frac{q}{kT} |\phi_s|\right) \right]^{1/2} - \left(\frac{\epsilon}{2\pi}\right)^{1/2} \frac{1}{q} \left[ \rho_d \left( |V_a| + |\psi_n| + |\phi_s| - \frac{kT}{q} \right) + \frac{kT}{q} q n_i \right]^{1/2} < p$$

and

$$\left(\frac{\epsilon}{2\pi}\right)^{1/2} \frac{1}{q} \left[ \rho_d \left( |V_a| + |\psi_n| - \frac{kT}{q} \right) + \frac{kT}{q} q n_i \exp\left(\frac{q}{kT} |\phi_s|\right) \right]^{1/2} - \left(\frac{\epsilon}{2\pi}\right)^{1/2} \frac{1}{q} \left[ \rho_d \left( |V_a| + |\psi_n| - \frac{kT}{q} \right) + \frac{kT}{q} q n_i \right]^{1/2} > p,$$

where  $p$  is the hole density per unit area, and the other parameters are constants of the sample as defined by Statz *et al.*<sup>21</sup> From the solution of these equations a set of curves is set up with the aid of a computer, yielding  $p$  as a function of  $\phi_s$  and  $V_a$ . The two limits for  $p$  are normally within 2%, and in the extreme values of  $\phi_s$  and  $V_a$ , it increases up to 5%, which is still within

experimental error, and well within the estimated error of the effective mobility calculation.

Together with the hole concentration at a given  $V_a$  and  $\phi_s$ , we must calculate the effective mobility as a function of  $V_a$  and  $\phi_s$ .

It is convenient to define Schrieffer's<sup>22</sup> expression  $\beta$  and  $B$  which are a function of  $V_a$  and  $\phi_s$  as follows:

$$\beta = \frac{1}{\mu p} \left( \frac{\epsilon}{8m^* n_i} \right)^{1/2} \exp\left(\frac{-q|\phi_s|}{2kT}\right),$$

$$B = \frac{\rho_d}{q n_i} \frac{q}{kT} \left[ |V_a| + |\psi_n| + |\phi_s| \right] \exp\left(\frac{-q|\phi_s|}{kT}\right),$$

where  $m^*$  was chosen as 0.25  $m_0$  consistent with Schrieffer. Schrieffer has calculated  $\mu_{\text{eff}}/\mu_{\text{bulk}}$  for  $\beta$  from 0.1 to 6 and  $B$  from 0 to 10. The authors extended this range to include values of  $\beta < 0.1$  and  $B > 10$  as required by the experimental observations. It is true that these calculations do not take into account the probable degeneracy of the surface. However, the consistency of our experimental results is good even though corrections for degenerate conditions were not made.

Thus a set of curves is drawn up (for a given sample) providing the effective mobility as a function of  $V_a$  and  $\phi_s$ . Combining  $p$  and the effective mobility, we thus obtain the surface conductivity  $\sigma_s$  as a function of  $V_a$  and  $\phi_s$  in a family of theoretical curves. From the experimental values of  $\sigma_s$  and  $V_a$ , the corresponding  $\phi_s$  is obtained from these curves.

Knowing  $V_a$  and  $\phi_s$ , we calculate  $N_s$  from Statz' equations and again obtain a family of theoretical curves relating  $N_s$  to  $\phi_s$  and  $V_a$ .

$$E_s^2 = \frac{8\pi}{\epsilon} \left[ \rho_d \left( |V_a| + |\psi_n| + |\phi_s| - \frac{kT}{q} \right) + q n_i \frac{kT}{q} \exp\left(\frac{q|\phi_s|}{kT}\right) \right]$$

and

$$Q = q N_s = \epsilon E_s / 4\pi.$$

The above calculations were made for both high- and low-resistivity "base" material by adjusting  $\psi_n$  and  $\rho_d$ . All calculations and measurements were made at room temperature.

Thus, with  $N_s$  and  $\phi_s$  calculated from the experimental results, the curves shown in the manuscript are obtained.